

Communication

All-Fiber In-Line Twist Sensor Based on a Capillary Optical Fiber

Qinghua Tang¹, Jiajian Ruan², Xiaojie Zuo¹, Zhongye Xie¹ and Xiaoyong Chen^{1,*} 

¹ School of Electrical Engineering and Intelligentization, Dongguan University of Technology, Dongguan 523808, China; qhtang4563@dgut.edu.cn (Q.T.); xiaojie@dgut.edu.cn (X.Z.); xiezy@dgut.edu.cn (Z.X.)

² Department of Physics, Shantou University, Shantou 515063, China; 18jjiang@stu.edu.cn

* Correspondence: xychen@dgut.edu.cn

Abstract: Twist sensors have emerged as crucial tools in the field of structural health monitoring, playing a significant role in monitoring and ensuring the integrity of critical infrastructure such as dams, tunnels, bridges, pipelines, and buildings. We proposed and demonstrated an all-fiber in-line twist sensor which was based on a capillary fiber spliced between two single-mode fibers with a transverse offset. Through a series of experiments, the sensor's performance was evaluated and quantified. The results showcased remarkable twist sensitivities in both clockwise and anticlockwise directions. With a transverse offset of 8.0 μm , the sensor exhibited twist sensitivities of $-0.077 \text{ dB}/^\circ$ and $0.043 \text{ dB}/^\circ$ in the clockwise and anticlockwise directions, respectively, in the measured twist range from 0 to 90° . Furthermore, it was also demonstrated that the sensor was temperature insensitive at the chosen wavelength of 1520 nm, which can assist in increasing measurement accuracy. Our sensor's low cost, simplicity of manufacture, and improved performance will push forward its adoption in future engineering applications such as structural health monitoring in dams, tunnels, and buildings.

Keywords: all-fiber interferometer; twist sensor; capillary fiber; sensitivity



Citation: Tang, Q.; Ruan, J.; Zuo, X.; Xie, Z.; Chen, X. All-Fiber In-Line Twist Sensor Based on a Capillary Optical Fiber. *Photonics* **2023**, *10*, 1052. <https://doi.org/10.3390/photronics10091052>

Received: 27 July 2023

Revised: 5 September 2023

Accepted: 14 September 2023

Published: 15 September 2023



Copyright: © 2023 by the authors. Licensee MDPI, Basel, Switzerland. This article is an open access article distributed under the terms and conditions of the Creative Commons Attribution (CC BY) license (<https://creativecommons.org/licenses/by/4.0/>).

1. Introduction

All-fiber in-line interferometers have garnered significant attention from researchers due to their numerous advantages, which include being low cost and easy to manufacture, as well as providing performance enhancement [1–3]. These interferometers have been extensively investigated for a wide range of applications, such as temperature sensing [4], strain sensing [5], refractive index sensing [6], and twist sensing [7], among others. Twist, being a crucial mechanical parameter, plays a vital role in structural health monitoring. The utilization of all-fiber twist sensors has witnessed a surge in various engineering applications. These sensors have proven invaluable in monitoring critical infrastructure including dams, tunnels, bridges, pipelines, and buildings [8]. The primary objective is to provide early warnings regarding potential abnormal conditions or impending accidents. By detecting twists at an early stage, casualties can be avoided, and prompt maintenance and repair advice can be provided.

The inherent advantages of all-fiber in-line interferometers make them an ideal choice for twist sensing in structural health monitoring [9]. Firstly, the low-cost nature of these devices ensures cost-effective deployment over a large-scale monitoring network. This affordability enables their widespread usage, facilitating the comprehensive monitoring of multiple structures simultaneously [10]. Additionally, the easy manufacturing process allows for quick production, making them readily available for immediate deployment. Furthermore, the performance improvement offered by all-fiber in-line interferometers is noteworthy. These sensors exhibit high sensitivity, enabling an accurate detection and measurement of twist in real time. The reliable and precise data obtained from these

sensors aid in assessing the structural integrity of various infrastructure components. This information is crucial for making informed decisions regarding maintenance and repairs, thereby increasing the overall safety and longevity of the structures [11].

A wide range of all-fiber in-line twist sensors based on different types of fibers has been reported, which includes multimode fibers (MMFs) [12], polarization-maintaining fibers (PMFs) [10], photonic crystal fibers (PCFs) [13,14], special fibers [15,16], and fiber gratings [17,18]. Each of these sensor types possesses its own set of advantages and disadvantages, making them suitable for different applications. For instance, twist sensors based on PCFs exhibit higher twist sensitivity compared to other fiber structures. However, these sensors come with the trade-off of complex signal interrogation systems and high manufacturing costs. The precise and accurate measurement capabilities of PCF-based sensors make them particularly suitable for applications requiring high sensitivity. On the other hand, twist sensors utilizing multimode fibers offer the advantages of straightforward structures and ease of implementation. These sensors are relatively simple to manufacture and can be readily integrated into existing systems, but they suffer from relatively lower twist sensitivity compared to other sensor types.

The capillary fiber, being the simplest structure among hollow fibers (or microstructure fibers), has received a lot of attention in recent years because of its benefits, such as its simple structure, flexibility, low invasiveness, and low cost of manufacture [19]. Capillary fibers are now being studied for different sensing domains, including the refractive index [20,21], temperature [22], liquid level [23,24], strain [25], pressure [26], and curvature [27]. However, the aforementioned capillary fiber applications necessitate that all fibers be aligned and twist-insensitive. In this research, we propose and investigate the properties of a capillary-fiber-based interferometer without fiber alignment for twist sensing. A capillary fiber is spliced between two single-mode fibers (SMFs) with a particular transverse offset to form the sensor. As a result of the transverse offset, several cladding modes, including noncircular symmetrical modes that are sensitive to twist, are excited in the capillary fiber wall, and they interfere with each other when they meet again in the lead-out SMF. Our proposed sensor is inexpensive, easy to construct, and straightforward to interrogate, making it suitable for future engineering applications such as structural health monitoring in dams, bridges, tunnels, and buildings.

2. Structure and Working Principle

The structure of our proposed all-fiber in-line interferometer, which is designed as a capillary fiber spliced between two SMFs with a specific transverse offset, can be seen in Figure 1. With the transverse offset, many high-order, noncircular symmetrical modes can be excited, leading to them propagating in the wall of the capillary fiber [28], and they can interfere with each other when they meet again at the end of the capillary fiber and are output through the lead-out SMF. According to the theory of the modal interference and assuming that the transverse offset between the lead-in SMF and the capillary fiber is d_1 , and that d_2 is between the capillary fiber and the lead-out SMF, the coupling coefficient based on the overlap integral method at the lead-in end ($L = 0$) and the lead-out end ($L = l$) can be written as follows [12]:

$$c_{nm}^{(0)} = \frac{|\int_0^\infty E_{lead-in}(r - d_1)\psi_{nm}^*(r)rdr|^2}{\int_0^\infty |E_{lead-in}(r)|^2rdr \int_0^\infty |\psi_{nm}^*(r)|^2rdr} \tag{1}$$

$$c_{nm}^{(l)} = \frac{|\int_0^\infty \psi_{nm}(r)E_{lead-out}^*(r - d_2)rdr|^2}{\int_0^\infty |E_{lead-out}(r)|^2rdr \int_0^\infty |\psi_{nm}(r)|^2rdr} \tag{2}$$

where $E_{lead-in}$ and $E_{lead-out}$ represent the electric field distribution of the lead-in and lead-out SMF, respectively, and Ψ_{nm} represents the electric field distribution of excited modes propagating in the capillary fiber.

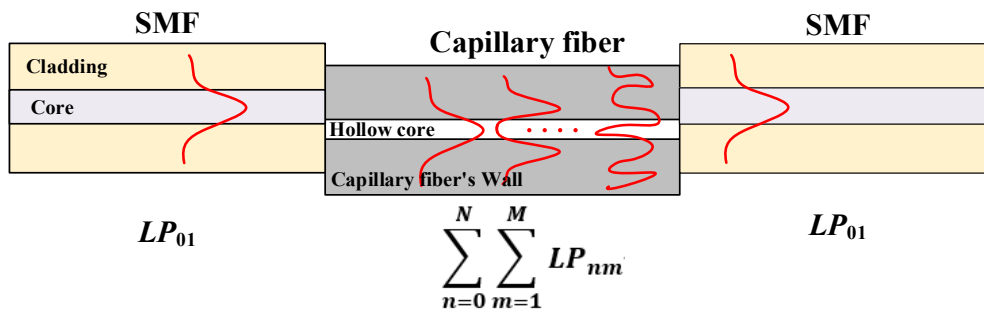


Figure 1. Structure of the proposed capillary-fiber-based all-fiber in-line interferometer. The red lines reflect the modes propagating in the fibers, whereas the dots represent other modes not depicted in this illustration.

According to the theory of coherent superposition in the interference of light, the output power of the proposed structure can be expressed as follows:

$$P_{out} = \sum_{n=0}^N \sum_{m=1}^M c_{nm}^{(0)} c_{nm}^{(l)} + 2 \sum_{n=0}^N \sum_{\substack{m=1 \\ nm \neq qp}}^M \sum_{q=0}^Q \sum_{p=1}^P \sqrt{c_{nk}^{(0)} c_{nk}^{(l)} c_{qp}^{(0)} c_{qp}^{(l)}} \cos(\varphi_{nm,qp}) \quad (3)$$

where $\varphi_{nm,qp}$ represents the phase difference between the modes LP_{nm} and LP_{qp} , and it can be written as $\varphi_{nm,qp} = l\Delta\beta_{nm,qp}$, which depends on the length of the capillary fiber, l , and the difference in the propagation constant, $\Delta\beta_{nm,qp}$. Assuming that both the lead-in and lead-out SMFs have the same structure and parameters, namely $d_1 = d_2 = d$ and $c_{nm}^{(0)} = c_{nm}^{(l)} = c_{nm}$, the output power of Equation (3) can be simplified as:

$$P_{out} = \sum_{n=0}^N \sum_{m=1}^M c_{nm}^2 + 2 \sum_{n=0}^N \sum_{\substack{m=1 \\ nm \neq qp}}^M \sum_{q=0}^Q \sum_{p=1}^P \sqrt{c_{nm}^2 c_{qp}^2} \cos(\varphi_{nm,qp}) \quad (4)$$

According to Equation (4), the proposed structure is based on multi-beam interference. Most of the power from the lead-in SMF can be coupled into high-order noncircular symmetrical modes in the capillary fiber with an appropriate transverse offset [12]. When this structure is twisted, the resulting refractive index disturbance along the capillary fiber causes a power exchange between these modes. As a result of this power exchange, the output power varies with the twist angle and orientation. Therefore, the proposed structure can be used for twist measurement.

3. Experimental System

Figure 2 depicts the experimental system for measuring twist. As the light source, we employed a broadband source (BBS) with a wavelength range from 1.5 to 1.6 m and a fiber interrogator (FS22DI, HBM FiberSensing, Darmstadt, Germany) with a resolution of 10 pm to capture the spectra. The SMFs were commercial standard SMFs that met the ITU-T G.652 requirements. The capillary fiber (TSP002150, Zhengzhou INNOSEP Scientific Co., Ltd., Zhengzhou, China) used in the experiment possessed inner and outer diameters of 2 and 138 μm , respectively, and had a length of 2 cm. The capillary fiber was spliced between two SMFs with a transverse offset of different values to analyze the spectral characteristics and twist response. To test the twist sensing application, a rotator (as shown in the inset in Figure 2) was positioned upstream of the proposed capillary-fiber-based interferometer, while a fiber clamp was installed downstream to clamp the fiber.

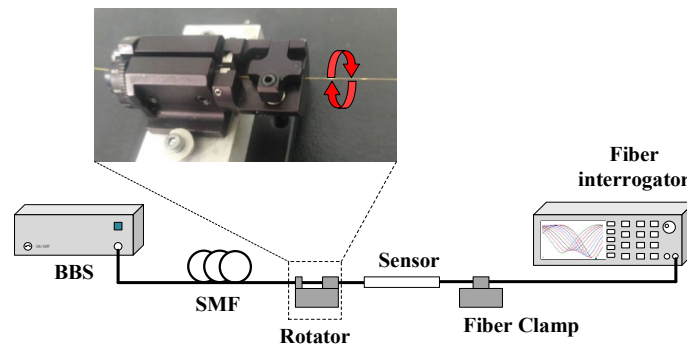


Figure 2. Experimental system for measuring twist.

4. Results and Discussion

We first investigated the twist response using our proposed sensor without a transverse offset, and the results are shown in Figure 3. The fiber twist-induced spectral response is small at the dip near 1570 nm. Although the measured range is 0–180, the linear range is only from 0 to 140°, with sensitivities of approximately 5.5×10^{-3} dB/° for twist in both the clockwise and anticlockwise directions. Moreover, the variation trends are the same under both twist directions. We need to explain two things: the resonant number and the poor linearity in the observed range. We think that the former is due to multi-beam interference in the capillary, and that when the phase differences between all propagating modes fit a particular condition, only one resonance is formed. For the latter, most of the power from the lead-in SMF is coupled into the excited circular symmetrical modes [29], and just a small amount of power is coupled into some low-order noncircular symmetrical modes that are stimulated randomly and are passively reliant on the capillary fiber topology. During the twist operation, the power exchange between the circular and noncircular modes is relatively minimal, and this power exchange is independent of the twist direction. As a result, when the sensor is twisted, the resonance strength fluctuates only a little with the rotation angle but has poor linearity.

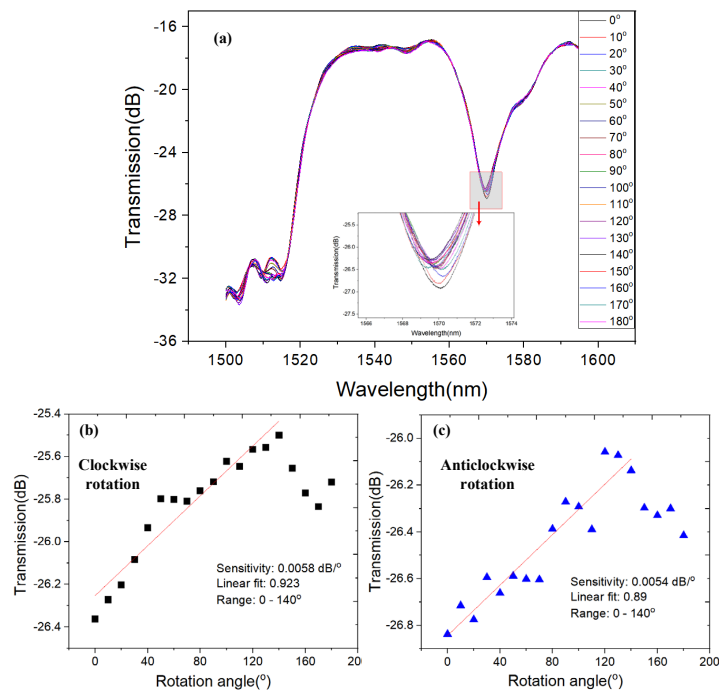


Figure 3. Measured results using the proposed sensor without a transverse offset: (a) spectral response; intensity variation at a wavelength of 1570 nm during the twist operated in (b) clockwise and (c) anticlockwise directions.

The experimental results for measuring twist using our sensor with a transverse offset of 5.5 and 8.0 μm are shown in Figures 4 and 5, respectively. As can be seen from Figure 4, only one dip appears in the measured wavelength range, and it shows opposite trends in variation during the twist operation in the clockwise and anticlockwise directions. The sensitivities are 0.035 and -0.031 $\text{dB}/^\circ$ in the clockwise and anticlockwise directions, respectively, with linearities larger than 0.998 in the measured twist range from 0 to 90° .

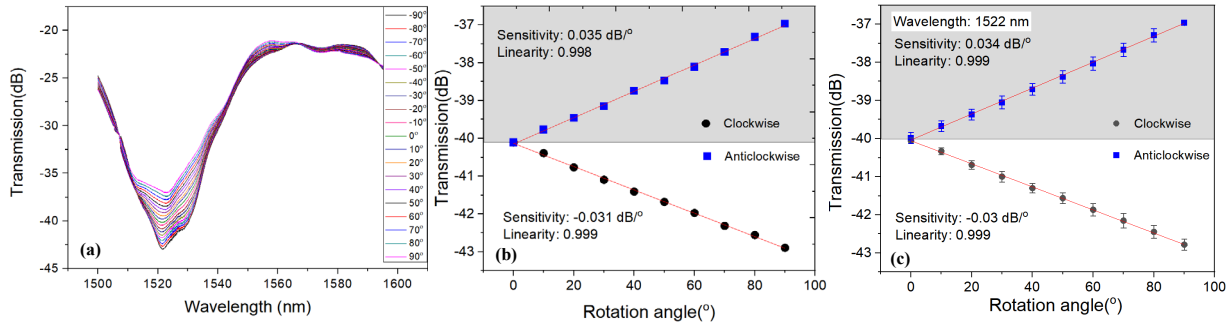


Figure 4. Measured results using the proposed sensor with a transverse offset of 5.5 μm : (a) spectral response; twist sensitivities at a wavelength of 1522 nm in clockwise (upper) and anticlockwise (down) directions of twist measured 1 time (b) and 5 times (c).

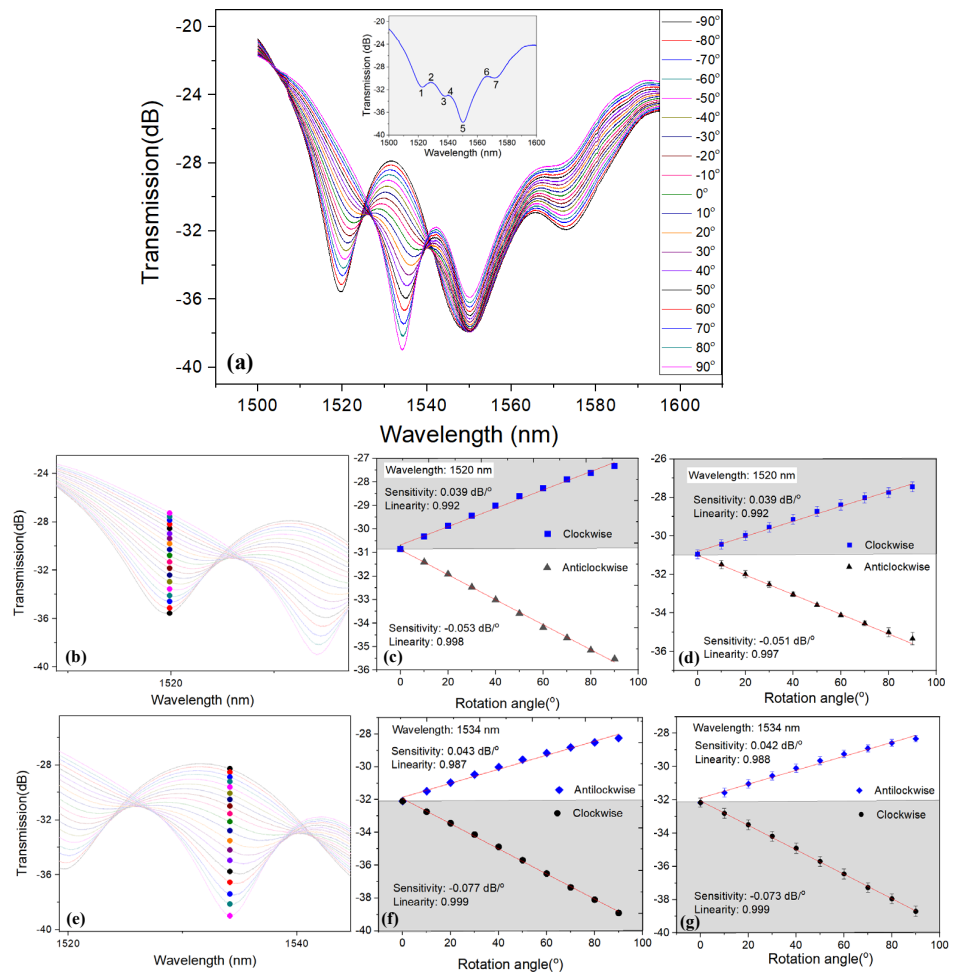


Figure 5. Measured results using the proposed sensor with a transverse offset of 8.0 μm : (a) spectral response; (b) intensity interrogation at wavelength of 1520 nm and the corresponding sensitivities measured 1 time (c) and 5 times (d); (e) intensity interrogation at wavelength of 1534 nm and the corresponding sensitivities measured 1 time (f) and 5 times (g).

When the transverse offset is 8.0 μm in our sensor, its spectrum can be seen in the inset in Figure 5a to have several peaks and valleys in the measured wavelength range. These peaks and valleys vary with the twist, and among them, valley 1 and peak 2 show obvious and regular variations, as presented in Figure 5a. In contrast to the traditional interrogation method of monitoring the wavelength shift or power variation of the center of a selective resonant dip or peak in the spectrum, we directly monitored the power variations at the selected wavelengths of 1520 (Figure 5b) and 1534 nm (Figure 5e), as they can provide the largest variations. Furthermore, because just a common laser source and a power meter are required for measurements, as compared to a broadband source and an optical spectrum analyzer which are required for conventional method, this interrogation approach can minimize costs and make the system easier to implement. The findings are depicted in Figure 5c,f. The sensitivities for the wavelengths of 1520 and 1534 nm are 0.039 and -0.077 dB/ $^\circ$, respectively, in the clockwise direction, while they are -0.053 and 0.043 dB/ $^\circ$ in the anticlockwise direction. The linearities are higher, being 0.98 in the measured range from 0 to 90 $^\circ$. It should be noted that the measured range in Figures 4 and 5 is 0–90 $^\circ$ rather than 0–180 $^\circ$, since when the twist angle exceeds 90 $^\circ$, the recorded spectra exhibit irregular fluctuations, making it difficult to summarize the varied trends at the monitored wavelengths using fitting lines. As a result, we may deduce that the measured range of our sensor for twist is 0 to 90 $^\circ$.

To investigate the sensor’s repeatability, we measured the twist five times, and the results are displayed in Figures 4c and 5d,g, and a column graph of sensitivities is presented in Figure 6. We can observe that the findings when measuring five times are identical to the results when measuring one time. The standard deviations of sensitivity are less than 1% and 4% for the transverse offsets of 5.5 and 8.0 μm , respectively. These results show that our sensor has high repeatability.

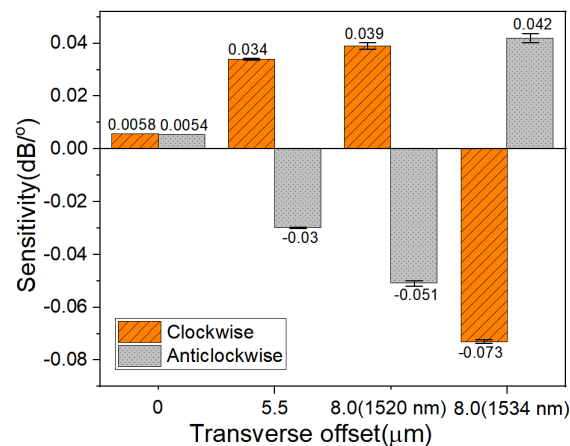


Figure 6. Comparison of twist sensitivities using the proposed sensor with different values of transverse offset.

Figure 6 summarizes the experimental results from Figure 3 to Figure 5, and we can see that the responses of the selected wavelengths depend on the twist directions and show opposite trends for the clockwise and anticlockwise orientations when a transverse offset is applied in the sensor. Owing to the transverse offset, some of the power is coupled into the excited noncircular symmetrical modes, and a power exchange occurs between these modes during the twist operation, thus resulting in spectral variations in accordance with the twist angles and orientations. Additionally, Figure 6 further indicates that the sensitivity of the sensor with a transverse offset is significantly greater than that without a transverse offset. Although Figure 6 demonstrates that raising the transverse offset from 5.5 to 8.0 m improves sensitivity, this does not imply that the sensitivity can be raised further with a significantly larger offset. We have also tested our sensor with offsets of 12 and

20 μm , and found that not only can the sensitivity not be improved further, but the loss also increases and the mechanical strength diminishes.

We also investigated the influence of temperature on our proposed sensor with a transverse offset of 8.0 μm , and the findings are presented in Figure 7. Although the power at the wavelength near 1553 nm clearly decreases as the temperature climbs from 25 to 65 $^{\circ}\text{C}$, the power variations at the selected wavelengths of 1520 and 1534 nm for twist sensing are fairly tiny, especially at 1520 nm which has a sensitivity of $-3.6 \times 10^{-5} \text{ dB}/^{\circ}\text{C}$. Because the temperature sensitivity at 1520 nm is a thousandth of what the fiber twist causes, we may disregard the temperature-induced cross-sensitivity when using the 1520 nm wavelength for the twist measurement. However, if we utilize the wavelength of 1534 nm for the twist measurement, we must ensure that the sensor operates in a temperature-controlled environment (the temperature sensitivity at 1534 nm is $-0.03 \text{ dB}/^{\circ}\text{C}$, which is comparable to the twist sensitivity) to ensure the validity of the measured data.

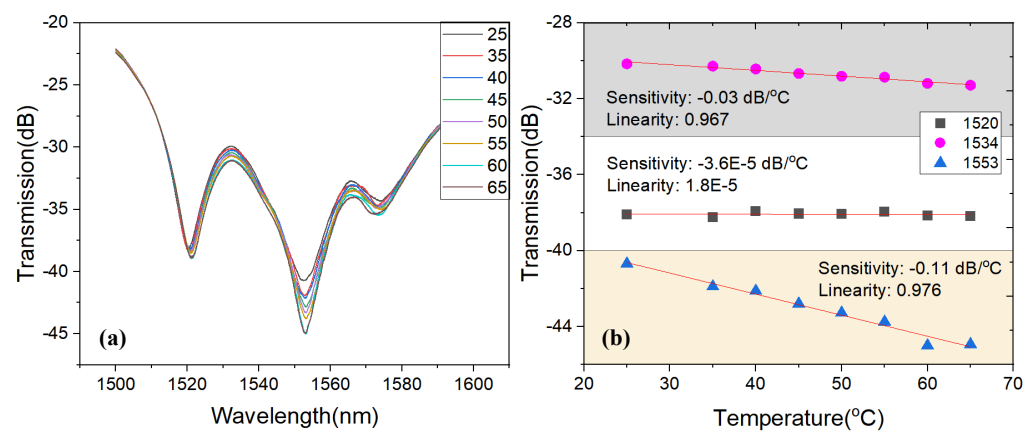


Figure 7. Measured results for temperature using the proposed sensor with a transverse offset of 8.0 μm : (a) spectral response; (b) sensitivities at the selected wavelengths of 1520, 1534, and 1553 nm.

In addition, at an offset of 8.0 μm , we investigated the axial strain-induced effect on the sensor, and the findings are given in Figure 8. The observed power at the wavelengths of 1520 and 1534 nm clearly fluctuates with the axial strain, and the trends fit two parabolas. To increase the measured accuracy, we should protect the sensor from axial strain, which reduces the strain-induced cross-sensitivity during practical measurements. Finally, it should be noted that introducing an offset during the splice would weaken the mechanical strength of the sensor. When the capillary and the SMF were aligned, the axial strain tolerance at the fusion site was $500 \pm 50 \mu\epsilon$. When the transverse offset was adjusted to 5.5 and 8.0 μm , the tolerable value dropped to 380 ± 50 and $150 \pm 20 \mu\epsilon$, respectively. Obviously, as the transverse offset grows, the mechanical strength of the axial strain decreases.

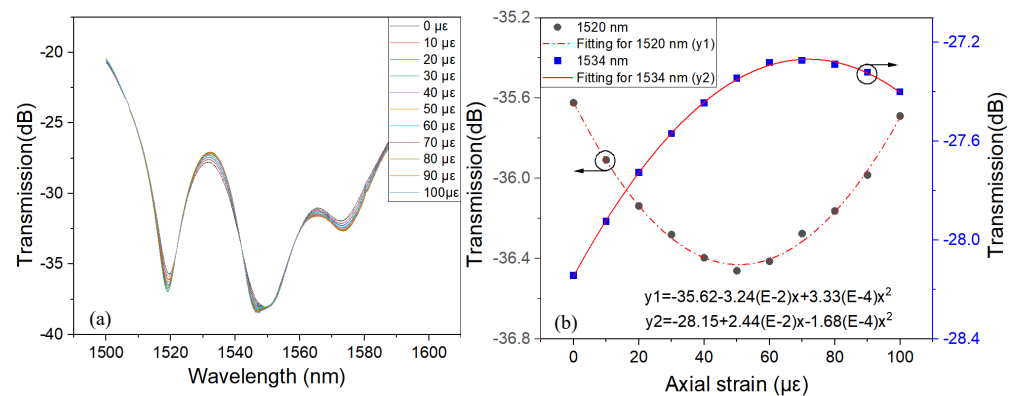


Figure 8. Measured results for axial strain using the proposed sensor with a transverse offset of 8.0 μm : (a) spectral response; (b) sensitivities at the selected wavelengths of 1520 and 1534 nm.

Table 1 compares our sensor to some other current twist sensors that have been reported. Although our sensor's performance (sensitivity and measured range) is not the finest among all of the sensors, it has the advantages of low cost, ease of manufacture, and simplicity of interrogation, making it a suitable alternative for practical measurement.

Table 1. Comparison with recently reported fiber-optic twist sensors.

Method	Sensitivity	Measured Range	Twist Direction Discrimination	Ref.
Two-Core Fiber	$-0.04 \text{ dB}/^\circ$	$-60\text{--}60^\circ$	Yes	[30]
LPG + TFBG	$1.074 \text{ dB}/(\text{rad}/\text{m})$	$-30\text{--}30^\circ$	No	[7]
PM-PCF	$0.014 \text{ dB}/^\circ$	$30\text{--}70^\circ$	No	[31]
Square-NCF	$0.11863 \text{ dB}/(\text{rad}/\text{m})$	$-360\text{--}360^\circ$	No	[32]
Fiber-optic MZI	$21.485 \text{ dB}/(\text{rad}/\text{cm})$	$-40\text{--}40 \text{ rad}/\text{m}$	Yes	[33]
Fiber Sagnac	$5.01 \text{ nm}/^\circ$	$370\text{--}400^\circ$	No	[34]
Dual-Core Fiber	$45.2 \text{ pm}/^\circ$	$-90\text{--}0^\circ$	Yes	[35]
Multimode fiber	$12 \text{ pm}/^\circ$	$0\text{--}90^\circ$	Yes	[12]
Taper-PMF	$0.077 \text{ nm}/^\circ$	$-180\text{--}180^\circ$	Yes	[36]
Seven-core fiber	$2.392 \text{ nm}/(\text{rad}/\text{m})$	$0\text{--}8 \text{ rad}/\text{m}$	Yes	[37]
Capillary fiber	$0.4 \text{ nm}/(\text{rad}/\text{m})$	$4.758\text{--}40.439 \text{ rad}/\text{m}$	Yes	[37]
	$0.073 \text{ dB}/^\circ$	$-180\text{--}180^\circ$	Yes	This work

5. Conclusions

We proposed and experimentally demonstrated a twist sensor based on a capillary fiber. A 2-cm-long capillary fiber was spliced between two SMFs with a transverse offset to create the sensor. Our sensor can give twist sensitivities of 0.035 and $-0.031 \text{ dB}/^\circ$ in the clockwise and anticlockwise directions, respectively, with a transverse offset of $5.5 \mu\text{m}$, and can give -0.077 and $0.043 \text{ dB}/^\circ$ with a transverse offset of $8.0 \mu\text{m}$, in a measured twist range from 0 to 90° . Furthermore, it was proved that our sensor was temperature-insensitive at the specified wavelength, which can aid in increasing the measurement accuracy. The combination of being low cost, easy to fabricate, and able to enhance performance will drive the use of our sensor in future engineering applications such as structural health monitoring in dams and tunnels.

Author Contributions: Writing—original draft preparation, Q.T.; investigation, J.R.; data analysis, X.Z.; validation, Z.X.; project administration and writing—review and editing, X.C. All authors have read and agreed to the published version of the manuscript.

Funding: This research was funded by the Guangdong Basic and Applied Basic Research Foundation, grant number 2021B1515140029, the Dongguan Science and Technology of Social Development Program, grant number 20221800905082, and the National Natural Science Foundation of China, grant numbers 62305056 and 62205057.

Institutional Review Board Statement: Not applicable.

Informed Consent Statement: Not applicable.

Data Availability Statement: All data are contained within the article.

Conflicts of Interest: The authors declare no conflict of interest.

References

- Liang, H.; Wang, J.; Zhang, L.; Liu, J.; Wang, S. Review of Optical Fiber Sensors for Temperature, Salinity, and Pressure Sensing and Measurement in Seawater. *Sensors* **2022**, *22*, 5363. [CrossRef]
- Chen, X.; Xu, J.; Zhang, X.; Guo, T.; Guan, B.O. Wide Range Refractive Index Measurement Using a Multi-Angle Tilted Fiber Bragg Grating. *IEEE Photonics Technol. Lett.* **2017**, *29*, 719–722. [CrossRef]
- Butt, M.A.; Kazanskiy, N.L.; Khonina, S.N.; Voronkov, G.S.; Grakhova, E.P.; Kutluyarov, R.V. A Review on Photonic Sensing Technologies: Status and Outlook. *Biosensors* **2023**, *13*, 568. [CrossRef]
- Tripathi, S.M.; Kumar, A.; Varshney, R.K.; Kumar, Y.B.P.; Marin, E.; Meunier, J.-P. Strain and Temperature Sensing Characteristics of Single-Mode–Multimode–Single-Mode Structures. *J. Light. Technol.* **2009**, *27*, 2348–2355. [CrossRef]

5. Lu, Z.; Liu, C.; Li, C.; Ren, J.; Yang, L. Ultra-High Sensitivity and Temperature-Insensitive Optical Fiber Strain Sensor Based on Dual Air Cavities. *Materials* **2023**, *16*, 3165. [[CrossRef](#)]
6. Shao, M.; Qiao, X.; Fu, H.; Li, H.; Jia, Z.; Zhou, H. Refractive Index Sensing of SMS Fiber Structure Based Mach-Zehnder Interferometer. *IEEE Photon. Technol. Lett.* **2014**, *26*, 437–439. [[CrossRef](#)]
7. Yang, K.; Liu, Y.; Wang, Z.; Li, Y.; Han, Y.; Zhang, H. Twist Sensor Based on Long Period Grating and Tilted Bragg Grating Written in Few-Mode Fibers. *IEEE Photonics J.* **2018**, *10*, 1–8. [[CrossRef](#)]
8. Li, H.-N.; Li, D.-S.; Song, G.-B. Recent applications of fiber optic sensors to health monitoring in civil engineering. *Eng. Struct.* **2004**, *26*, 1647–1657. [[CrossRef](#)]
9. Budinski, V.; Donlagic, D. Fiber-Optic Sensors for Measurements of Torsion, Twist and Rotation: A Review. *Sensors* **2017**, *17*, 443. [[CrossRef](#)]
10. Huang, B.; Shu, X. Highly Sensitive Twist Sensor Based on Temperature- and Strain-Independent Fiber Lyot Filter. *J. Light. Technol.* **2017**, *35*, 2026–2031. [[CrossRef](#)]
11. Lesnik, D.; Donlagic, D. In-line, fiber-optic polarimetric twist/torsion sensor. *Opt. Lett.* **2013**, *38*, 1494–1496. [[CrossRef](#)]
12. Chen, X.; Guan, R.; Horche, P.R. Transverse Offset Based Single-Multi-Single Mode Fiber Structure for Vector Rotation Sensing. *J. Light. Technol.* **2019**, *37*, 2726–2733. [[CrossRef](#)]
13. Hu, T.; Zhao, Y.; Wu, D. Novel torsion sensor using a polarization maintaining photonic crystal fiber loop mirror. *Instrum. Sci. Technol.* **2016**, *44*, 46–53. [[CrossRef](#)]
14. Nalawade, S.M.; Harnol, S.S.; Thakur, H.V. Temperature and Strain Independent Modal Interferometric Torsion Sensor Using Photonic Crystal Fiber. *IEEE Sens. J.* **2012**, *12*, 2614–2615. [[CrossRef](#)]
15. Liu, D.; Kumar, R.; Wei, F.; Han, W.; Mallik, A.K.; Yuan, J.; Yu, C.; Kang, Z.; Li, F.; Liu, Z.; et al. Highly sensitive twist sensor based on partially silver coated hollow core fiber structure. *J. Light. Technol.* **2018**, *36*, 3672–3677. [[CrossRef](#)]
16. Yu, D.; Mo, Q.; Hong, Z.; Fu, S.; Sima, C.; Tang, M.; Liu, D. Temperature-insensitive fiber twist sensor based on elliptical-core few-mode fiber. *Opt. Lett.* **2016**, *41*, 4617–4620. [[CrossRef](#)]
17. Guo, T.; Liu, F.; Guan, B.O.; Albert, J. Polarimetric multi-mode tilted fiber grating sensors. *Opt. Express* **2014**, *22*, 7330–7336. [[CrossRef](#)]
18. Yiping, W.; Wang, M.; Huang, X. In fiber Bragg grating twist sensor based on analysis of polarization dependent loss. *Opt. Express* **2013**, *21*, 11913–11920. [[CrossRef](#)]
19. Sarker, N.; Kaysir, M.R.; Jahirul Islam, M. Modal analysis of capillary optical fibers and their possible applications in sensing. In Proceedings of the 2019 IEEE International Conference on Telecommunications and Photonics (ICTP), Dhaka, Bangladesh, 28–30 December 2019.
20. Zhang, X.; Shao, H.; Yang, Y.; Pan, H.; Pang, F.; Wang, T. Refractometry with a Tailored Sensitivity Based on a Single-Mode-Capillary-Single-Mode Fiber Structure. *IEEE Photonics J.* **2017**, *9*, 1–8. [[CrossRef](#)]
21. Pereira, D.; Bierlich, J.; Kobelke, J.; Ferreira, M.S. Hybrid sensor based on a hollow square core fiber for temperature independent refractive index detection. *Opt. Express* **2022**, *30*, 17754–17766. [[CrossRef](#)]
22. Yu, Y.; Zhang, X.; Wang, K.; Wang, Z.; Sun, H.; Yang, Y.; Deng, C.; Huang, Y.; Wang, T. Coexistence of transmission mechanisms for independent multi-parameter sensing in a silica capillary-based cascaded structure. *Opt. Express* **2021**, *29*, 27938–27950. [[CrossRef](#)] [[PubMed](#)]
23. Roldán-Varona, P.; Pérez-Herrera, R.A.; Rodríguez-Cobo, L.; Reyes-González, L.; López-Amo, M.; López-Higuera, J.M. Liquid level sensor based on dynamic Fabry-Perot interferometers in processed capillary fiber. *Sci. Rep.* **2021**, *11*, 3039. [[CrossRef](#)] [[PubMed](#)]
24. Huang, Z.; Liu, D.; Wu, Q.; Tian, K.; Zhao, H.; Shen, C.; Farrell, G.; Semenova, Y.; Wang, P. Light transmission mechanisms in a SMF-capillary fiber-SMF structure and its application to bi-directional liquid level measurement. *Opt. Express* **2022**, *30*, 21876–21893. [[CrossRef](#)]
25. Pan, H.; Zhang, X.; Yan, M.; Wang, J.; Shao, H.; Pang, F.; Huang, S.; Wang, T. Strain sensing characteristics based on a fiber-capillary-fiber Fabry-Perot interferometer. In Proceedings of the 2017 Conference on Lasers and Electro-Optics Pacific Rim (CLEO-PR), Singapore, 31 July–4 August 2017.
26. Salceda-Delgado, G.; Newkirk, A.V.; Antonio-Lopez, J.E.; Martinez-Rios, A.; Schülzgen, A.; Amezcua-Correa, R. Optical Capillary Fiber Mode Interferometer for Pressure Sensing. *IEEE Sens. J.* **2020**, *20*, 2253–2260. [[CrossRef](#)]
27. Zhu, C.; Zhuang, Y.; Huang, J. Machine Learning Assisted High-Sensitivity and Large-Dynamic-Range Curvature Sensor Based on No-Core Fiber and Hollow-Core Fiber. *J. Light. Technol.* **2022**, *40*, 5762–5767. [[CrossRef](#)]
28. Sun, W.; Zhang, X.; Yu, Y.; Yang, L.; Hou, F.; Yang, Y.; Wang, T. Comparative Study on Transmission Mechanisms in a SMF-Capillary-SMF Structure. *J. Light. Technol.* **2020**, *38*, 4075–4085. [[CrossRef](#)]
29. Liu, D.; Li, W.; Wu, Q.; Ling, F.; Tian, K.; Shen, C.; Wei, F.; Farrell, G.; Semenova, Y.; Wang, P. Strain-, curvature- and twist-independent temperature sensor based on a small air core hollow core fiber structure. *Opt. Express* **2021**, *29*, 26353–26365. [[CrossRef](#)]
30. Song, Z.; Li, Y.; Hu, J. Directional Torsion Sensor Based on a Two-Core Fiber with a Helical Structure. *Sensors* **2023**, *23*, 2874. [[CrossRef](#)] [[PubMed](#)]
31. Fu, H.Y.; Khijwania, S.K.; Tam, H.Y.; Wai, P.K.A.; Lu, C. Polarization-maintaining photonic-crystal-fiber-based all-optical polarimetric torsion sensor. *Appl. Opt.* **2010**, *49*, 5954–5958. [[CrossRef](#)]

32. Song, B.; Miao, Y.; Lin, W.; Zhang, H.; Wu, J.; Liu, B. Multi-mode interferometer-based twist sensor with low temperature sensitivity employing square coreless fibers. *Opt. Express* **2013**, *21*, 26806–26811. [[CrossRef](#)]
33. Ren, Y.; Liu, X.; Zhang, X.; Yang, J. Two-mode fiber based directional torsion sensor with intensity modulation and 0° turning point. *Opt. Express* **2019**, *27*, 29340–29349. [[CrossRef](#)] [[PubMed](#)]
34. Htein, L.; Gunawardena, D.S.; Liu, Z.; Tam, H.-Y. Two semicircular-hole fiber in a Sagnac loop for simultaneous discrimination of torsion, strain and temperature. *Opt. Express* **2020**, *28*, 33841–33853. [[CrossRef](#)] [[PubMed](#)]
35. Cheng, T.; Li, B.; Zhang, F.; Liu, W.; Chen, X.; Gao, Y.; Yan, X.; Zhang, X.; Wang, F.; Suzuki, T.; et al. Measurement A Sagnac Interferometer-Based Twist Angle Sensor Drawing on an Eccentric Dual-Core Fiber. *J. Light. Technol.* **2022**, *71*, 1–8.
36. Zhou, Q.; Zhang, W.; Chen, L.; Yan, T.; Zhang, L.; Wang, L.; Wang, B. Fiber torsion sensor based on a twist taper in polarization-maintaining fiber. *Opt. Express* **2015**, *23*, 23877–23886. [[CrossRef](#)]
37. Liu, C.; Jiang, Y.; Du, B.; Wang, T.; Feng, D.; Jiang, B.; Yang, D. Strain-insensitive twist and temperature sensor based on seven-core fiber. *Sens. Actuators A Phys.* **2019**, *290*, 172–176. [[CrossRef](#)]

Disclaimer/Publisher’s Note: The statements, opinions and data contained in all publications are solely those of the individual author(s) and contributor(s) and not of MDPI and/or the editor(s). MDPI and/or the editor(s) disclaim responsibility for any injury to people or property resulting from any ideas, methods, instructions or products referred to in the content.